TEMPERATURE-PROGRAMMED HYDROGENATION OF SURFACE CARBONACEOUS DEPOSITS ON A Ni/SiO_2 METHANATION CATALYST

Vladimír STUCHLÝ and Karel KLUSÁČEK

Institute of Chemical Process Fundamentals,
Czechoslovak Academy of Sciences, 165 02 Prague 6-Suchdol

Received April 3, 1989
Accepted May 11, 1989

Hydrogenation of surface carbonaceous deposits from CO disproportionation or methanation on a high-weight loading commercial Ni/SiO_2 catalyst was investigated by temperature programmed surface reaction (TPSR). Two types of surface carbon (C_α and C_β) were hydrogenated following the CO disproportionation. Adsorbed carbon monoxide was probably hydrogenated after CO methanation. Hydrogenation of C_α proceeded substantially faster than hydrogenation of C_β and faster than hydrogenation of preadsorbed CO. Significantly lower activation energy was estimated for hydrogenation of C_α than for hydrogenation of CO (50 vs 90 kJ/mol). An approach for analysis of the data from a temperature programmed experiment is given.

Methanation has been employed for many years to remove traces of CO and CO_2 from hydrogen in ammonia plants. Methanation is also a promising reaction for production of substitute natural gas (SNG) from coal and flared CO (refs[1,2]). Though this conversion is not yet economically justified, methanation has been the subject of numerous studies. It was demonstrated that the reaction of CO with H_2 proceeds on Ni catalysts either via CH_nO surface complexes or via a surface carbon. The formation or conversion of these surface intermediates to CH_4 is believed to determine the rate of methanation at most conditions[3-6].

A valuable insight into the methanation has been provided by non-stationary kinetic measurements, i.e. by transient response experiments and temperature programmed techniques[6-15]. It was evidenced that various forms of surface CO and C with different reactivity to hydrogen exist on a nickel surface. Their nature and reactivity were found to depend strongly on the support and nickel loading. Either C or CO are assumed to be hydrogenated during the CO methanation.

The aim of this work has been to evaluate forms of surface carbonaceous deposits on the commercial methanation catalyst G-33. The method of temperature programmed surface reaction (TPSR) has been used to obtain a kinetic description of hydrogenation of carbonaceous species deposited under CO disproportionation or methanation. An approach for evaluation of data from a temperature programmed experiment is given. A curve-fitting procedure instead of a single-point method (e.g. heating rate variation) has been applied to kinetic analysis[16-19].

THEORETICAL

Model. During CO methanation and disproportionation the surface of Ni catalyst is populated mainly by surface C and CO (refs[11,13,14]). The following reactions can thus take place after exposure of used catalyst to hydrogen during TPSR (s is a surface site):

$$Cs + 2\,H_2 \rightarrow CH_4 + s \qquad (A)$$

or

$$COs + 3\,H_2 \rightarrow CH_4 + H_2O + s \qquad (B)$$

The aim was to distinguish if reaction (*A*) or reaction (*B*) proceeds during TPSR after CO disproportionation and methanation. Reaction (*A*) and (*B*) were supposed to be irreversible and it was assumed that CH_4 is not readsorbed[10,12]. It is also supposed that water and methane desorb simultaneously[3] while CO does not desorb (separate experiments). For the sake of simplicity hydrogen is formally written as reacting from the gaseous phase although it is probably preadsorbed at the beginning of a temperature programmed experiment and reacts from the surface[8]. This assumption does not change the results of quantitative data analysis.

The dynamics of reaction (*A*) or (*B*) in a nonisothermal isobaric CSTR is described by a set of ordinary differential equations for the gaseous phase:

$$dp_i/dt = p_i^0 F^0 T/(VT^0) - p_i^0 F/V + R_i WRT/V \quad i = 1, 2, 3, 4 \qquad (1)$$

and for the catalyst surface

$$dq_j/dt = R_j \quad j = 5, 6, 7\,. \qquad (2)$$

The temperature of feed, T^0, remains constant while the reactor temperature is increased, e.g. linearly

$$dT/dt = b\,. \qquad (3)$$

The rate of reaction (*A*) or (*B*) can be expressed in terms of the formal power-type kinetic equation as

$$r_k = k_k q_j^g p_2^h \quad k = \mathrm{I}, \mathrm{II}\,; \quad j = 5, 6\,. \qquad (4)$$

The temperature dependence of a kinetic constant is given by Arrhenius relation

$$k_k = A_k \exp(-E_k/RT) \quad k = \mathrm{I}, \mathrm{II}\,. \qquad (5)$$

Since it can be written that

$$\Delta S_k = R \ln A_k\,, \qquad (6)$$

an entropy factor, ΔS_k, instead of the pre-exponential factor, A_k, was introduced into Eq. (5) to accelerate the convergence of the numerical computation

$$k_k = \exp\left[(\Delta S_k - E_k/T)/\boldsymbol{R}\right]. \tag{7}$$

Rates of formation of individual reaction components are given by

$$R_i = a_{i,k} r_k \quad i = 1, 2 \ldots 7\,; \quad k = \mathrm{I}, \mathrm{II}\,, \tag{8}$$

where $a_{i,k}$ are stoichiometric coefficients of the i-th component in the reaction (A) or (B).

The outlet flowrate, F, generally differs from the inlet flowrate, F^0, due to the reaction stoichiometry and due to the dynamics of adsorption and desorption steps. Relevant relations were derived elsewhree[20]. However, for higher flowrates and lower heating rates (used in this work), the effect of reaction stoichiometry and adsorption-desorption dynamics is small and can be neglected. Then, the outlet flowrate depends only on the reactor temperature

$$F = F^0 T/T^0\,. \tag{9}$$

Combination of the Eqs (1), (3) and (9) leads to the dynamic balance of CH_4 ($i = 3$) under transient conditions of a TPSR

$$\mathrm{d}p_3/\mathrm{d}t = (p_3^0 \,\mathrm{M}\, p_3)\, F^0 T/(bVT^0) + R_3 \boldsymbol{WRT}/(bV)\,. \tag{10}$$

As the feed does not contain methane ($p_3^0 = 0$) and it holds that

$$R_3 = -b\,\mathrm{d}q_j/\mathrm{d}T \quad j = 5, 6\,, \tag{11}$$

from Eqs (10) and (11) we obtain

$$\mathrm{d}p_3/\mathrm{d}T = -F^0 T/(bVT)\, p_3 - \mathrm{d}q_j/\mathrm{d}T \boldsymbol{WRT}/V \quad j = 5, 6\,, \tag{12}$$

where

$$\mathrm{d}q_j/\mathrm{d}T = -(1/b) \exp\left[(\Delta S_k - E_k/T)/\boldsymbol{R}\right] q_j^{\mathrm{g}} p_2^{\mathrm{h}} \quad k = \mathrm{I}, \mathrm{II}\,. \tag{13}$$

Eqs (12) and (13) are complemented by the initial conditions

$$\text{for} \quad T = T^0 \quad q_j = q_j(T^0) \qquad p_3 = 0\,. \tag{14}$$

Eqs (12)–(14) represent the dynamic model of the TPSR technique used in this work.

To obtain the initial guesses of unknown parameters (ΔS_j, E_j, q_j, g, h; $j = 5, 6$) of the ordinary differential equations (ODE) (*13*) it is useful to solve an algebraic version of Eqs (*12*) and (*13*). The numerical values of derivative dp_3/dT in Eq. (*12*) are small in comparison with the right-hand side values and they can be neglected. Eqs (*12*) and (*13*) then yield

$$0 = \boldsymbol{WR} \exp\left[(\Delta S_k - E_k/T)/\boldsymbol{R}\right] q_j^g p_2^h - p_3 F^0/T^0 \qquad (15)$$

The validity of this assumption was tested numerically and only slight differences were found when using the dynamic model (Eqs (*12*)–(*14*)) and its simplified version (Eq. (*15*)).

Numerical procedure. Estimation of parameters ΔS_k, E_k and q_k of ODE's (*12*) and (*13*) was facilitated by solving the simplified algebraic model (*15*) and matching the computed and experimental data. Parameters u and h were fixed at 0, 1, or 2. The quality of fitting the experimental profiles was evaluated by means of the least-squares criterion and using a Marquardt–Levenberg minimization strategy. The exact solution was obtained in the second step by solving the differrential model (*12*) and (*13*) for ΔS_k, E_k and q_k with parameters from the solution of algebraic model as initial estimates while again minimizing the least-square objective function. A 4th order Runge–Kutta method with self-adjusting step size control was used for solving the initial value problem. Confidence limits of parameters were computed as constant Chi-square boundary limits.

EXPERIMENTAL

Experiments were performed in an ideally mixed flow reactor (CSTR) described elsewhere[20]. The mass and heat transfer effects could be neglected under our TPSR conditions. All gases were purified catalytically prior to use in order to remove oxygen and water impurities. 100 mg of the crushed Ni/SiO_2 catalyst (G-33, Girdler-Sudchemie GmbH, F.R.G., see Table I) was placed in the reactor, heated in a flow of hydrogen (30 ml/min) to 673 K and reduced at this temperature for 2 hours. The catalyst was then purged with nitrogen (15 ml/min, 0·5 h) and cooled to the temperature of pretreatment (300, 478 or 528 K). CO from mixtures with N_2 or H_2 (molar ratio 1 : 5, total flowrate 40 ml/min) was subsequently preadsorbed for 0·5 h (steady-state). The catalyst temperature was decreased to 300 K in N_2 and the temperature programmed experiment was started in the flow of pure hydrogen, nitrogen or their mixtures (60 ml/min). The rate of temperature increase was typically 10 K/min. The reaction product CH*g* was analyzed periodically using an on-line gas chromatograph (TCD, 2-m column packed with Carbosphere, 90°C, 40 ml/min H_2).

RESULTS

Two sets of experiments were carried out either in the presence of hydrogen (CO methanation) or in its absence (CO disproportionation). After 30 min of either

reaction the feeding of reactants was stopped, the reaction mixture was replaced by nitrogen and the catalyst was in about 2 min cooled down to ambient temperature. No CO desorbed from the catalyst during the cooling period and the final surface composition thus corresponded to the reaction conditions. Surface carbonaceous deposits were subsequently hydrogenated in a TPSR run.

TPSR following the CO disproportionation. Hydrogenation of surface carbonaceous deposits produced methane. Dependence of CH_4 partial pressure on the catalyst temperature is given in Fig. 1. The data are for preadsorption of CO at 300, 478 and 528 K. The results are also summarized in Table II. TPSR profiles of CH_4 are characterized by one or two peaks depending on the temperature of disproportionation (preadsorption). After an exposure at 300 K a distinct methane peak was seen at 475 K. For the run at 478 K methane was evolved with a maximum at 450 K (peak α). A small peak (β) appeared at about 635 K. Hydrogenation of deposits from the run at 528 K proceeded similarly but the high-temperature peak was slightly shifted to lower temperature (620 K). Above 650 K all samples evolved CH_4 with rising intensity. This part of CH_4 profiles was due to hydrogenation of less reactive carbon species the hydrogenation of which cannot contribute significantly to methane formation at 478 and 528 K. From Fig. 1 it can be seen that the amount of CH_4 formed below 650 K rose when the temperature of CO disproportionation was increased.

This is evidenced in Table II where kinetic parameters of the first peaks from Fig. 1 are also summarized. As our measurements were carried out in excess of hydrogen, separate experiments were needed to determine the dependence of hydrogenation rate on the hydrogen partial pressure. Both samples from the 300 and the 478 K were examined. No differences were observed in CH_4 profiles when decreasing the pressure of H_2 from 100 to 10 kPa. This gives evidence about the zero-order

TABLE I
Properties of the G-33 catalyst

Ni loading[a], wt. %	29
Surface area[b], m^2/g	112
Particle diameter, mm	0·16—0·25
Pore volume[b], cm^3/g	0·134
Bulk density[c], g/cm^3	1·73
Apparent density[c], g/cm^3	2·84
Helium density, g/cm^3	3·10
Porosity	0·52
Most frequent pore radius[b], nm	40

[a] Gravimetry, [b] BET method, [c] mercury porosimetry.

dependence on hydrogen pressure. Profiles of methane were then fitted with the assumption of the first-order kinetics with respect to the concentration of surface

TABLE II

Summary of the TPSR measurements on the G-33 catalyst

Temperature K	Peak temperature[a], K		Peak area μmol/g		Rate constant[b] min	Activation energy, kJ mol^{-1}
	α	β	α	β[c]	α	α
			CO disproportionation			
300	475	—	60	—	$(1{\cdot}3 \pm 0{\cdot}1) \cdot 10^9$	86 ± 2
478	450	435	294	10	$(1{\cdot}5 \pm 0{\cdot}1) \cdot 10^5$	49 ± 1
528	450	420	356	24	$(2{\cdot}5 \pm 0{\cdot}1) \cdot 10^5$	51 ± 1
			CO methanation			
300	475	—	84	—	$(5{\cdot}0 \pm 0{\cdot}2) \cdot 10^9$	91 ± 2
478	475	—	108	—	$(6{\cdot}0 \pm 0{\cdot}2) \cdot 10^9$	91 ± 2
528	475	—	101	—	$(1{\cdot}2 \pm 0{\cdot}1) \cdot 10^{10}$	94 ± 2

[a] α and β correspond to the first and second peak in a methane profile, [b] first-order kinetics, [c] approximate values.

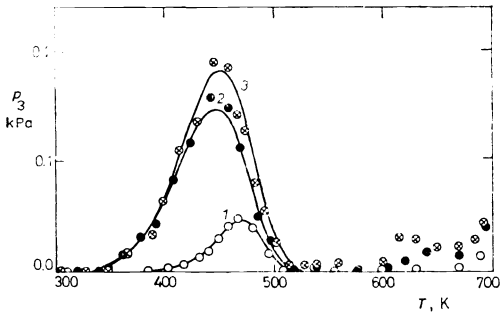

FIG. 1

Methane partial pressure as a function of temperature during the TPSR of the samples from CO disproportionation at 300 K (curve *1*, ○), 478 K (*2*, ●) and 528 K (*3*, ⊗). The curves were computed according to the model (*12*) and (*13*)

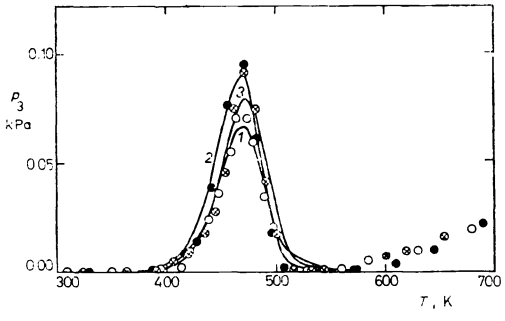

FIG. 2

Methane partial pressure as a function of temperature during the TPSR of the samples from CO methanation at 300 K (curve *1*, ○), 478 K (*2*, ●) and 528 K (*3*, ⊗). The curves were computed as in Fig. 1

component. The quality of the fit can be judged from Fig. 1. In Table II significant differences in activation energies can be revealed for the sample treated at 300 K and the samples treated at 478 and 528 K (86 and 50 kJ/mol, respectively). Activation energies for the 478 and 528 K samples were almost the same. The low intensity of the methane peak and strong overlapping above 528 K during the TPSR prevented the analysis of second peaks of the 478 and 528 K samples.

TPSR following the CO methanation. Results are presented in Fig. 2 for 300, 478 and 528 K samples and summarized in Table II. Only one distinct methane peak was observed. After methanation at 300 K methane appeared in a peak with peak temperature of 475 K. Following the exposures at 478 K and 528 K methane was again detected with maximum at about 475 K. All samples exhibited CH_4 formation above 528 K due to hydrogenation of less reactive deposits. As can be judged from Fig. 2, only minor differences were observed in the amount of methane formed from 300, 478 and 528 K samples. In Table II peak areas, pre-exponential factors and activation energies of peaks from Fig. 2 are given. All the values are very near as expected from the similarity of curves in Fig. 2. Activation energies of about 90 kJ/mol were always found.

DISCUSSION

Hydrogenation of Carbonaceous Deposits from CD *Disproportionation*

A comparison with literature has been made to evaluate consistency of our data with previous results on nickel catalysts and to determine the chemical nature of compounds hydrogenated during our TPSR measurements. McCarty and Wise[12] have carried out TPSR experiments on a related commercial high-temperature methanation catalyst G-65 which contains similar amount of Ni as G-33 used here (25 vs 29%) and differs in additives to prevent sintering.

McCarty and Wise[12] admitted pulses of CO in helium at 300, 550 and 610 K. After exposure of the G-65 catalyst to CO at 300 K, one peak of methane was observed with a peak temperature considerably higher than for samples treated at higher temperature. On 550 and 610 K samples they found two methane peaks which corresponded to hydrogenation of surface α and β carbon, respectively. The α carbon was considered to represent isolated surface carbon atoms and was hydrogenated at a sufficiently fast rate to be a likely intermediate in nickel-catalyzed methanation. β Caron was less reactive (activation energy 130 vs 71 kJ/mol for α) and was taken as amorphous surface carbon.

In our work, hydrogenation of carbonaceous deposits from CO disproportionation proceeded similarly except of the increasing methane signal above 528 K. Only one distinct peak was detected following the exposure at 300 K and at higher temperature than was the temperature for the samples treated at 478 and 528 K (Fig. 1). Sub-

stantially higher activation energy was estimated for hydrogenation of deposits after exposure at 300 K than at 478 and 528 K (86 vs 50 kJ/mol, see Table II). Kester et al.[9] have shown that hydrogenation of the low-temperature deposits (from exposure at 300 K) was not due to hydrogenation of a surface carbon but was due to hydrogenation of CO. As we have not observed CO disproportionation at 300 K (separate experiments) and the estimated activation energy of 86 kJ/mol agrees well with previously published results[10] we conclude that adsorbed CO was hydrogenated on the G-33 catalyst treated at 300 K.

The hydrogenation of surface carbonaceous species following the CO disproportionation at 478 and 528 K (Fig. 1) revealed two types of carbonaceous deposits, in agreement with McCarty and Wise[12]. Unlike their work[12] lower amount of less reactive carbon (probably β carbon[12]) was observed on our samples treated at 478 and 528 K. We also estimated lower activation energy for hydrogenation of α carbon than McCarty and Wise (50 vs 71 kJ/mol). One would expect a decrease in the activation energy, however, since we used the low-temperature catalyst with a higher methanation activity. Our results are thus more consistent with the activation energies of 41–44 kJ/mol reported by Ozdogan et al.[10]. These authors ascribed the peaks in their TPSR profiles to hydrogenation of surface C similarly as McCarty and Wise[12]. Since CO disproportionated on our catalyst above 500 K we conclude that unlike the sample treated at 300 K, at 478 and at 528 K the surface carbon in two forms was formed on the G-33 catalyst.

Hydrogenation of Carbonaceous Deposits from CO *Methanation*

In contrast to hydrogenation of carbonaceous deposits from CO disproportionation only one peak was detected after CO methanation, irrespective to the methanation temperature (Fig. 2). The peak exhibited always the same position on the temperature axis and approximately the same activation energy of 90 kJ/mol (Table II). The methane profiles remind of that observed by Zagli et al.[8] on the G-65 catalyst after pretreatment of their catalyst by CO in flowing hydrogen. A similar peak was seen on a 19% Ni/Al_2O_3 catalyst saturated by pulses of CO in hydrogen[7]. Ozdogan et al.[10] reported two methane peaks with activation energies of 83–19 and 97 to 107 kJ/mol, respectively. They used a 10·5% Ni/Al_2O_3 catalyst, however, on which two forms of CO are hydrogenated[7,9]. Nevertheless, these values of activation energies agree well with our values. The authors[7–10] ascribed their methane peaks to hydrogenation of CO.

We can conclude that though CO was hydrogenated on our catalyst at 478 and 528 K and not at 300 K (separate experiments) adsorbed CO was probably hydrogenated in the following TPSR experiments. This conclusion is supported by the fact that nickel surface is covered mainly by CO during the methanation on Ni/SiO_2. The surface coverage by C is relatively low[14].

On the other hand, Goodman et al.[21] estimated that surface carbon populated about one half of nickel surface at molar ratio $H_2/CO = 4$ and 528 K. Hayes and Ward[11] deduced from their infrared spectroscopic measurements that surface carbon was hydrogenated during their TPSR runs. Magnetic measurements suggested also the presence of significant ammounts of surface carbidic species[22]. Underwood and Bennett[13] performed transient response experiments on a 10% Ni/Al_2O_3 catalyst and arrived to the conclusion that both surface carbon and carbon monoxide were hydrogenated after CO methanation.

Our results support the conclusion that CO rather than C is hydrogenated on the G-33 catalyst in the CO methanation. Caron was hydrogenated after the CO disproportionation and much more easier than carbon monoxide. Estimated activation energies of both processes lie well within the values reported in literature which indicates the feasibility of kinetic analysis of TPSR data using the curve-fitting procedure.

SYMBOLS

$a_{i,k}$	stoichiometric coefficient of the i-th component in the k-th reaction
A_k	pre-exponential factor of the k-th reaction, min^{-1}
b	heating rate, K/min
E_k	activation energy of the k-th reaction, kJ/mol
F	volumetric flowrate, cm^3/min
k_k	kinetic constant of the k-th reaction, min^{-1}
p_i	partial pressure of the i-th gaseous component, kPa
q_j	concentration of the j-th surface component, μmol/g
r_k	rate of the k-th reaction, μmol/(min g)
R_i	rate of formation of the i-th component, μmol/(min g)
R	gas constant, kJ/(mol K)
ΔS_k	entropy factor of the k-th reaction, kJ/(mol K)
t	time, min
T	temperature, K
V	void reactor volume, cm^3
W	catalyst weight, g

Subscripts

i	gaseous reaction component (1 ≡ CO, 2 ≡ H_2, 3 ≡ CH_4, 4 ≡ H_2O)
j	surface reaction component (5 ≡ COS, 6 ≡ CS, 7 ≡ S)
k	reaction

Superscript

°	reactor inlet

REFERENCES

1. Frost A. C., Elek L. F., Yang Ch.-L., Rəbo J. A.: Energy Progr. *2*, 247 (1982).
2. Frost A. C., Elek L. F., Rabo J. A.: U.S. Patent 4,400,575 (1983).
3. Vanice M. A.: Catal. Rev.-Sci. Eng. *14*, 153 (1973).
4. Araki M., Ponec V.: J. Catal. *44*, 439 (1976).
5. Ho S. V., Harriott P.: J. Catal. *64*, 272 (1980).
6. Bartholomew C. H.: Catal. Rev.-Sci. Eng. *24*, 67 (1982).
7. Kester K. B., Zagli E., Falconer J. L.: Appl. Catal. *22*, 311 (1986).
8. Zagli E., Falconer J. L., Keenan C. A.: J. Catal. *46*, 453 (1976).
9. Kester K. B., Falconer J. L.: J. Catal. *89*, 380 (1984).
10. Ozdogan S. Z., Gochis P. D., Falconer J. L.: J. Catal. *83*, 257 (1983).
11. Lee P.-I., Schwarz J. A.: Ind. Eng. Chem., Process Des. Dev. *25*, 76 (1986).
12. McCarty J. G., Wise H.: J. Catal. *57*, 406 (1979).
13. Underwood R. P., Bennett C. O.: J. Catal. *86*, 245 (1984).
14. Hayes R. E., Ward K. J.: Appl. Catal. *20*, 123 (1986).
15. Biloen P., Helle J. N., Van Den Berg I. G. A., Sachtler W. M. H.: J. Catal. *81*, 450 (1983).
16. Pisani C., Rabino G., Ricca F.: Surf. Sci. *41*, 277 (1977).
17. Monti D. A. M., Baiker A.: J. Catal. *83*, 323 (1983).
18. Ehrhardt K., Richter M., Roost V., Öhlmann G.: Appl. Catal. *17*, 23 (1985).
19. Stuchlý V., Klusáček K.: Appl. Catal. *34*, 263 (1987).
20. Samková J., Klusáček K., Schneider P.: Collect. Czech. Chem. Commun. *51*, 2761 (1986).
21. Goodman J. G., Kelley R. D., Madey T. E., White J. M.: J. Catal. *64*, 479 (1980).
22. Mirodatos C., Dalmon J. A., Martin G. A.: *Catalysis on the Energy Scene, Proceedings of the 9th Canadian Symposium on Catalysis, Quebec, Oct. 1984 Elsevier.*

Translated by the author (V.S.).